# Optimizing of the piezo-optic interaction geometry in SrB$_4$O$_7$ crystals

OLEH BURYY[1*], NATALIYA DEMYANYSHYN[2], BOHDAN MYTSYK[2], ANATOLIY ANDRUSHCHAK[1]

[1] Institute of Telecommunications, Radioelectronics and Electronic Engineering,
  Lviv Polytechnic National University, 12 Bandery St., Lviv, 79013, Ukraine

[2] Karpenko Physico-Mechanical Institute of NAS of Ukraine,
  5 Naukova St., Lviv, 79060, Ukraine

*Corresponding author: oburyi@polynet.lviv.ua

The optimal geometries of the piezo-optic interaction are determined for SrB$_4$O$_7$ crystals by the extreme surfaces method. The goal functions of optimization are the change of optical path length and optical path difference, normalized on mechanical stress and crystal thickness, and the parameters of optimization are the spherical angles determining the directions of the light beam propagation and the uniaxial pressure action. It is shown that the maximal changes of optical path length for the orthogonal polarized waves are equal to 2.09 or 1.65 B (1 B = 1 brewster = $10^{-12}$ m$^2$/N) and the maximal change of optical path difference is equal to 2.22 B respectively in transversal geometry of the piezo-optic interaction (for $\lambda$ = 633 nm and $T$ = 20°C).

Keywords: piezo-optical effect, optical path, path difference, SrB$_4$O$_7$ crystals.

## 1. Introduction

Piezo-optic effect, *i.e.*, the changes of the refractive indices caused by the mechanical stress, is often used in polarization-optical [1−4] and interferometric [5, 6] modulators as well as in different modulator-based devices. The most efficient operation of such modulators can be achieved by the optimization of the piezo-optical effect geometry, *i.e.*, by defining of such mutual orientations of electromagnetic wave and the applied uniaxial pressure that ensure the maximal value of the effect.

This optimization can be realized by the analysis of indicative surfaces, which represent the spatial distribution of the piezo-optic (*e.g.*, see [7–9]), electro-optic [10, 11] or acousto-optic [12, 13] effect. However, this optimization is incomplete because it allows determining the maxima of the stress-induced refractive index changes, whereas the parameters describing the modulation efficiency of optical material are the change in the optical path (for the interferometric modulators) or the change in the path dif-

ference (for the polarization-optical modulators). The optimization of these parameters can be carried out by the construction and the analysis of the extreme surfaces [14] representing all possible maxima of the effect for different spatial orientations of the light propagation direction or internal influence action. Herewith all possible extrema of the optical path/path difference changes are taken into account.

Here we use this method for determination of the piezo-optical interaction optimal geometry for the case of the biaxial $SrB_4O_7$ crystal (point group *mm*2) interesting for applications due to its high radiation resistance and transparence in UV spectral region up to 130 nm [15]. The same approach is planned to be applied in future for other crystalline materials, particularly, for low symmetry TMA-CuCl$_4$ [16], Gly-H$_3$PO$_4$ [17], Cs$_2$HgCl$_4$ [18, 19] crystals which reveal good acousto-optical and/or piezo-optical properties, *i.e.*, low sound velocities, high elasto-optical and piezo-optical coefficients, *etc*.

## 2. Method for calculating

The extreme surfaces are constructed in two possible ways dependent on the parameters of optimization, namely the components of the unit vector of light propagation or the unit vector of direction of the applied uniaxial pressure. Particularly, the extreme surface of the mechanical stress is obtained when spherical angles defining the directions of the applied uniaxial pressure $\theta_\sigma$, $\varphi_\sigma$ are the parameters of optimization and the angles which determine the directions from the origin to the points of the surface coincide with the angles $\theta_k$, $\varphi_k$ defining the light propagation. Contrary, if the angles $\theta_k$, $\varphi_k$ are the parameters of optimization and the angles $\theta_\sigma$, $\varphi_\sigma$ define the points on the surface, the corresponding surface is the wave vector one.

The numerical Levenberg–Marquardt' method [20] is used for optimization and the algorithm used for construction of the extreme surfaces is the following:

1) required elastic, optical, piezo-optical parameters of the crystal are defined;

2) the set of angles $\theta$, $\varphi$ used for construction of the extreme surface is defined; in the case of the mechanical stress extreme surface $\theta = \theta_k$, $\varphi = \varphi_k$, in the case of the wave vector extreme surface $\theta = \theta_\sigma$, $\varphi = \varphi_\sigma$;

3) in each point defined in point (2): the optimization is realized in accordance with the expression of the objective function (see below); the varied parameters of optimization are the angles $\theta_\sigma$, $\varphi_\sigma$ in the case of the mechanical stress extreme surface or $\theta_k$, $\varphi_k$ in the case of the wave vector one;

4) the extreme surface is constructed in accordance with the maximal values of the objective function determined in point (3).

Only one type of the extreme surface, *i.e.*, the mechanical stress or the wave vector one, is enough for determination of the optimal geometry of induced interaction. However, for higher generality as well as for checking of our results here we present the calculations for both types of the surfaces. Obviously, the optimal geometries obtained by the analysis of mechanical stress and wave vector surfaces must coincide.

Moreover, for higher generality of the optimization, its objective function is formulated in following ways.

*The objective function $\pi'_{i\sigma}$* – the effective piezo-optic coefficient $\pi'_{i\sigma} = 2\delta n_i/(\sigma n_i^3)$ as it is followed from the expression describing the piezo-optic effect $\delta n_i = (\pi_{i\sigma}\sigma n_i^3)/2$ for the changes of the refractive index under the influence of the mechanical stress $\sigma$ [21, 22].

The dependence of this value on the directions of the light polarization and the applied pressure is investigated in [21]; the obtained expression for $\pi'_{i\sigma}$ is

$$\frac{2}{\sigma n^3}\,\delta n(\theta_i,\,\varphi_i,\,\theta_\sigma,\,\varphi_\sigma) \;=\; \pi'_{i\sigma} \;=$$

$$= \left[\pi_{11}\sin^2(\theta_\sigma)\cos^2(\varphi_\sigma) + \pi_{12}\sin^2(\theta_\sigma)\sin^2(\varphi_\sigma) + \pi_{13}\cos^2(\theta_\sigma)\right]\sin^2(\theta_i)\cos^2(\varphi_i) +$$

$$+ \left[\pi_{21}\sin^2(\theta_\sigma)\cos^2(\varphi_\sigma) + \pi_{22}\sin^2(\theta_\sigma)\sin^2(\varphi_\sigma) + \pi_{23}\cos^2(\theta_\sigma)\right]\sin^2(\theta_i)\sin^2(\varphi_i) +$$

$$+ \left[\pi_{31}\sin^2(\theta_\sigma)\cos^2(\varphi_\sigma) + \pi_{32}\sin^2(\theta_\sigma)\sin^2(\varphi_\sigma) + \pi_{33}\cos^2(\theta_\sigma)\right]\cos^2(\theta_i) +$$

$$+ 0.5\left[\pi_{44}\sin(\varphi_\sigma)\sin(\varphi_i) + \pi_{55}\cos(\varphi_\sigma)\cos(\varphi_i)\right]\sin(2\varphi_\sigma)\sin(2\varphi_i) +$$

$$+ 0.5\,\pi_{66}\sin^2(\theta_\sigma)\sin(2\varphi_\sigma)\sin^2(\theta_i)\sin(2\varphi_i)$$

$$(1)$$

where $\pi_{lm}$ are the piezo-optical coefficients (POCs) indicated in Table 1, $\theta_i$, $\varphi_i$ are the angles of the spherical coordinate system determining the direction of light polarization, and $\theta_\sigma$, $\varphi_\sigma$ are the angles determining the direction of the applied pressure $\sigma$.

The optimization with the objective function $\pi'_{i\sigma}$ was carried out for comparison with the results obtained in [21].

T a b l e  1. The parameters of SrB₄O₇ crystals used in the calculations ($\lambda = 632.8$ nm and $T = 20$°C; 1 B = 1 brewster = $10^{-12}$ m²/N).

| Parameter | Value | Reference |
|---|---|---|
| The main refractive indices ($\lambda = 632.8$ nm) | $n_1 = 1.7333$, $n_2 = 1.7323$, $n_3 = 1.7356$ | [24] |
| Piezo-optic coefficients [B] ($\lambda = 632.8$ nm) | $\pi_{11} = -0.29$, $\pi_{12} = 0.55$, $\pi_{13} = 0.37$, $\pi_{21} = 0.47$, $\pi_{22} = -0.20$, $\pi_{23} = 0.36$, $\pi_{31} = 0.56$, $\pi_{32} = 0.52$, $\pi_{33} = -0.37$, $\pi_{44} = -0.35$, $\pi_{55} = -0.53$, $\pi_{66} = -0.42$ | [24] |
| Elastic compliance coefficients [$10^{-12}$ m²/N] | $S_{11} = 3.54$, $S_{12} = -0.86$, $S_{13} = -0.33$, $S_{22} = 4.05$, $S_{23} = -0.48$, $S_{33} = 2.76$, $S_{44} = 7.19$, $S_{55} = 8.33$, $S_{66} = 7.52$ | Calculated from values of elastic coefficients $C_{mn}$ determined in [25] |

*The objective function* $\delta'\Delta_{k,\,max}$ – the change in the optical path for $n_{k,\,max}$. This function is written for the largest refractive index $n_{k,\,max}$ (of the two refractive indices for the wave propagating in **k** direction) on the basis of the known expression [22]

$$\delta\Delta_{k,\,max} = \delta(n_{k,\,max}t_k) - \delta t_k = (\delta n_{k,\,max}t_k + n_{k,\,max_0}\delta t_k) - \delta t_k =$$

$$= (n_{k,\,max} - n_{k,\,max_0})t_k + (n_{k,\,max_0} - 1)\delta t_k \tag{2}$$

where $\delta n_{k,\,max} = n_{k,\,max} - n_{k,\,max_0}$, and $t_k$ is the sample thickness in the direction of light propagation.

Dividing both sides of Eq. (2) by the thickness $t_k$ and uniaxial stress (uniaxial pressure) $\sigma$, one obtains the objective function

$$\delta'\Delta_{k,\,max} = \frac{\delta\Delta_{k,\,max}}{\sigma t_k} = \sigma^{-1}\left|(n_{k,\,max} - n_{k,\,max_0}) + (n_{k,\,max_0} - 1)\frac{\delta t_k}{t_k}\right| \tag{3}$$

where the modulus is written for better graphical visualization of the results. This function describes the optical path change per the unit of the thickness and the unit of the mechanical stress; the index "0" corresponds to zero pressure, $\delta t_k/t_k$ is the relative extension in **k** direction. This value can be written as [23]

$$\frac{\delta t_k}{t_k} = \tilde{\mathbf{k}}\hat{\varepsilon}\mathbf{k} = \tilde{\mathbf{k}}\hat{S}\hat{\sigma}\mathbf{k} = \sigma(\varepsilon_1 k_1^2 + \varepsilon_2 k_2^2 + \varepsilon_3 k_3^2 + \varepsilon_4 k_2 k_3 + \varepsilon_5 k_1 k_3 + \varepsilon_6 k_1 k_2) \tag{4}$$

where $\tilde{\mathbf{k}}$ is the wave vector **k** in the contravariant basis, $\hat{\varepsilon}$ is the tensor of deformation with components $\varepsilon_v = \Sigma_{\mu=1}^6 S_{\mu v}\sigma_\mu$, $\hat{S}$ is the tensor of the elastic compliance coefficients (its components are indicated in Table 1), $\hat{\sigma}$ is the tensor of the mechanical stress, in the case of the uniaxial pressure applied along $\mathbf{q}_\sigma$ direction it is equal to $\hat{\sigma} = \sigma\mathbf{q}_\sigma\mathbf{q}_\sigma$. Because the components of the unit vector $\mathbf{q}_\sigma$ are $q_1 = \sin(\theta_\sigma)\cos(\varphi_\sigma)$, $q_2 = \sin(\theta_\sigma)\sin(\varphi_\sigma)$, $q_2 = \cos(\theta_\sigma)$ in the spherical coordinate system, the components of $\hat{\sigma}$ can be written as [7]: $\sigma_1 = \sigma\sin^2(\theta_\sigma)\cos^2(\varphi_\sigma)$, $\sigma_2 = \sigma\sin^2(\theta_\sigma)\sin^2(\varphi_\sigma)$, $\sigma_3 = \cos^2(\theta_\sigma)$, $\sigma_4 = \sigma\sin(\theta_\sigma)\cos(\theta_\sigma)\sin(\varphi_\sigma)$, $\sigma_5 = \sigma\sin(\theta_\sigma)\cos(\theta_\sigma)\cos(\varphi_\sigma)$, and $\sigma_6 = \sigma\sin^2(\theta_\sigma)\sin(\varphi_\sigma)\cos(\varphi_\sigma)$.

The refractive indices of the orthogonally polarized waves are determined from the Fresnel equation [23]. In the case of biaxial media its roots are

$$n_{max,\,min}^{-2} = A \pm \sqrt{A^2 - B - C} \tag{5}$$

where

$$A = 0.5\left[(\eta_{22} + \eta_{33})k_1^2 + (\eta_{11} + \eta_{33})k_2^2 + (\eta_{11} + \eta_{22})k_3^2\right] +$$

$$- \eta_{12}k_1 k_2 - \eta_{13}k_1 k_3 - \eta_{23}k_2 k_3 \tag{5a}$$

$$B = -(\eta_{22}\eta_{33} - \eta_{23}^2)k_1^2 - (\eta_{11}\eta_{33} - \eta_{13}^2)k_2^2 - (\eta_{11}\eta_{22} - \eta_{12}^2)k_3^2 \tag{5b}$$

$$C = -2(\eta_{13}\eta_{23} - \eta_{12}\eta_{33})k_1 k_2 - 2(\eta_{12}\eta_{23} - \eta_{22}\eta_{13})k_1 k_3 +$$
$$- 2(\eta_{12}\eta_{13} - \eta_{11}\eta_{23})k_2 k_3 \tag{5c}$$

and $\eta_{ik}$ are the components of the tensor of the dielectric impenetrability (polarization constants). Their changes under the mechanical stress are described by the expressions [22, 23]

$$\Delta\eta_{ij} \equiv \Delta\eta_{\mu} = \pi_{ijkl}\sigma_{kl} \equiv \pi_{\mu\nu}\sigma_{\nu} \tag{6}$$

where $\pi_{ijkl} = \pi_{\mu\nu}$ are the POCs. The refractive index $n_{k,\,max}$ corresponds to the sign "–" in Eqs. (5a)–(5c).

*The objective function* $\delta'\Delta_{k,\,min}$ – the change in the optical path for $n_{k,\,min}$,

$$\delta'\Delta_{k,\,min} = \frac{\delta\Delta_{k,\,min}}{\sigma t_k} = \sigma^{-1}\left|(n_{k,\,min} - n_{k,\,min_0}) + (n_{k,\,min_0} - 1)\frac{\delta t_k}{t_k}\right| \tag{7}$$

where $n_{k,\,min}$ is smaller of the two refractive indices for the wave propagating in **k** direction.

*The objective function* $\delta'\Delta_k$ – the change in the propagation difference for the orthogonally polarized waves

$$\delta'\Delta_k = \frac{\delta(\Delta n_k t_k)}{\sigma t_k} = \frac{\delta\Delta_k}{\sigma t_k} =$$
$$= \sigma^{-1}\left|(n_{k,\,max} - n_{k,\,max_0}) - (n_{k,\,min} - n_{k,\,min_0}) + (n_{k,\,max_0} - n_{k,\,min_0})\frac{\delta t_k}{t_k}\right| \tag{8}$$

where $\Delta n_k$ is the birefringence.

The parameters of SrB$_4$O$_7$ crystal used in our calculations are indicated in Table 1.

## 3. Results of calculations

*Objective function – the effective piezo-optic coefficient* $\pi'_{i\sigma}$ *determined by Eq. (1).* This calculation is carried out for checking of the correctness of the method used for the investigation. Because the effective piezo-optic coefficient is determined by the polarization of the light wave (by the angles $\theta_i$, $\varphi_i$), not by the direction of its propagation, the polarization extreme surface was built instead of the surface of the wave vector (Fig. 1**a**). The angles $\theta_i$, $\varphi_i$ are the parameters of the optimization in this case. The mechanical stress extreme surface obtained after optimization on the angles $\theta_\sigma$, $\varphi_\sigma$ is shown in Fig. 1**b**. As it is shown by the optimization, the maximal value of the effective piezo-optic coefficient $\pi'_{i\sigma}$ is achieved for the light wave polarized along
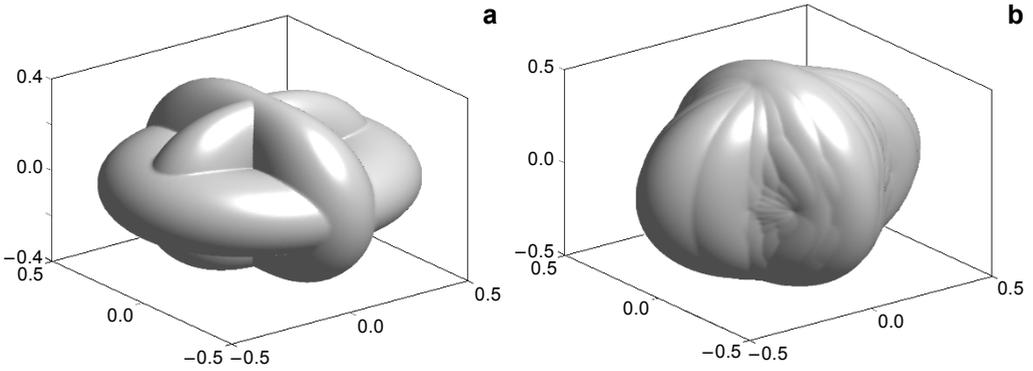
Fig. 1. The extreme surfaces of the light polarization (**a**) and the mechanical stress (**b**) for the objective function $\pi'_{i\sigma}$ (all values are in brewsters).

$X_3$ axis of the crystal ($\theta_i = 0$) and pressure applied perpendicular to $X_3$ ($\theta_\sigma = 90°$, $\varphi_\sigma = 0$). The corresponding maximal value of $\pi'_{i\sigma}$ is equal to $\pi_{31} = 0.56$ B (1 B = = 1 brewster = $10^{-12}$ m$^2$/N) that coincides with the result obtained in [21].
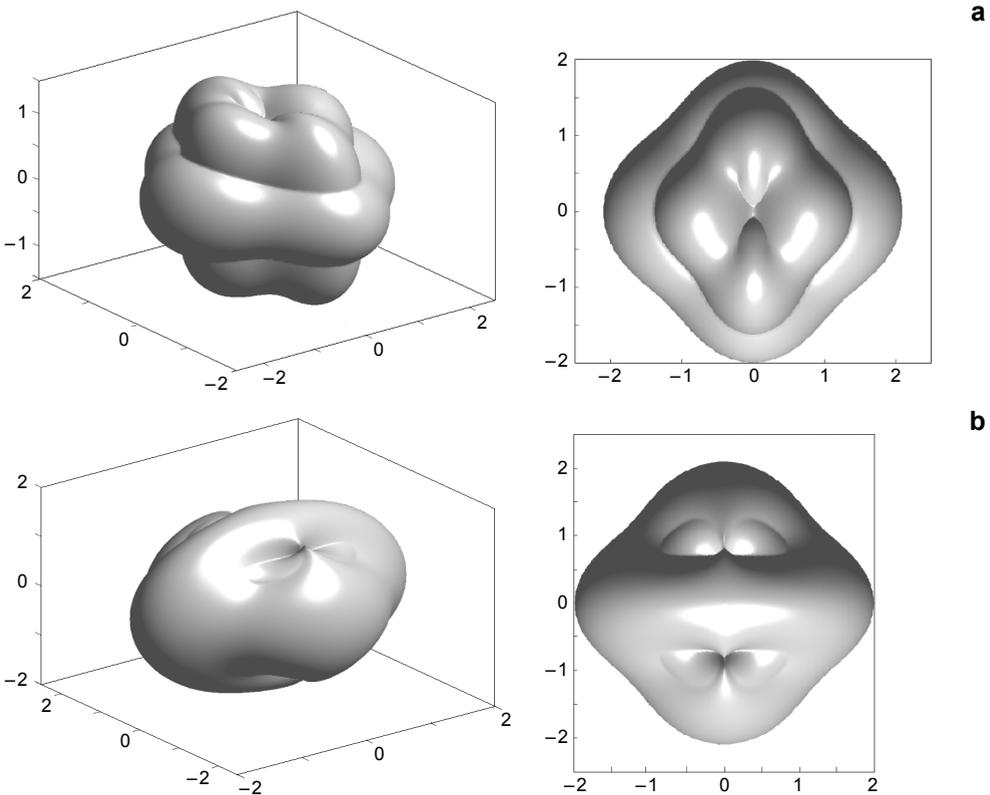


Fig. 2. The extreme surfaces of the wave vector (**a**) and the mechanical stress (**b**) for the objective function $\delta'\Delta_{k,\,max}$ (all values are in brewsters); the right images are the top views of corresponding surfaces.

*Objective function* $\delta'\Delta_{k,\,max}$ *determined by Eq. (3)*. The extreme surfaces for this case are shown in Fig. 2. As it is followed from the analysis of the surfaces, the maximal change in the optical path $\delta'\Delta_{k,\,max}$ is equal to 2.09 B. This value is realized for the direction of light propagation defined by the angles $\theta_k = 90°$, $\varphi_k = 90°$ and the direction of the applied pressure $\theta_\sigma = 90°$, $\varphi_\sigma = 0$, *i.e.*, in the transversal geometry of interaction.

*Objective function* $\delta'\Delta_{k,\,min}$ *determined by Eq. (7)*. The extreme surfaces for this case are shown in Fig. 3. The maximal value of the optical path change for $n_{k,\,min}$ is equal to 1.65 B and realized for the light propagation direction defined by the angles $\theta_k = 147°$, $\varphi_k = 90°$ and the direction of the applied pressure $\theta_\sigma = 90°$, $\varphi_\sigma = 0$, *i.e.*, in the transversal geometry as well as in the previous case.

*Objective function* $\delta'\Delta_k$ *determined by Eq. (8)*. The extreme surfaces of the wave vector and the mechanical stress for this objective function are shown in Fig. 4.

The maximal value of the propagation difference for the orthogonally polarized waves $\delta'\Delta_k$ is equal to 2.22 B and realized for the light propagation direction defined by the angles $\theta_k = 90°$, $\varphi_k = 90°$ and the direction of the applied pressure $\theta_\sigma = 90°$, $\varphi_\sigma = 0$, *i.e.*, in the exactly transversal geometry of interaction.
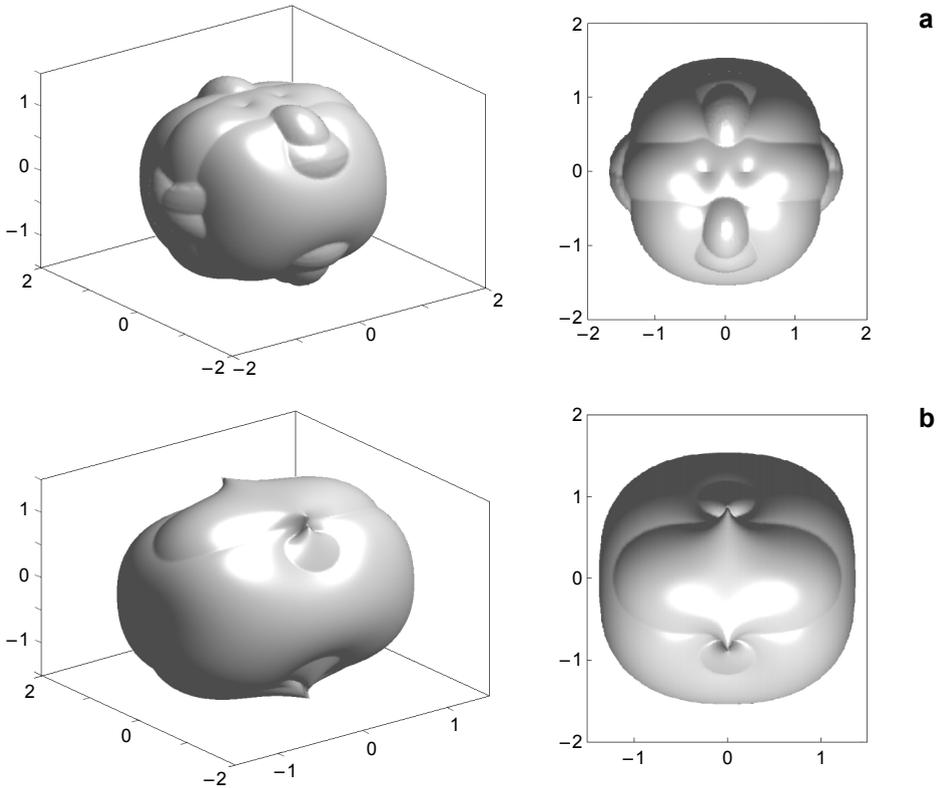


Fig. 3. The extreme surfaces of the wave vector (**a**) and the mechanical stress (**b**) for the objective function $\delta'\Delta_{k,\,min}$ (all values are in brewsters); the right images are the top views of corresponding surfaces.

Fig. 4. The extreme surfaces of the wave vector (**a**) and the mechanical stress (**b**) for the objective function $\delta'\varDelta_k$ (all values are in brewsters); the right images are the top views of corresponding surfaces.

The results of optimization for all considered objective functions are collected in Table 2 for the convenience of comparison. The directions of light wave polarization are also indicated in Table 2.

## 4. Discussion

As it is followed from the analysis for the objective functions $\delta'\varDelta_{k,\,\mathrm{max}}$, $\delta'\varDelta_{k,\,\mathrm{min}}$ and $\delta'\varDelta_k$ the maximal achievable changes of the optical path and the propagation differ-

T a b l e  2. The maximal values of the objective functions and their corresponding angles.

| Objective function | Direction of propagation | | Direction of polarization | Direction of uniaxial | Maximal |
| | $\theta_k$ [deg] | $\varphi_k$ [deg] | $\theta_i,\ \varphi_i$ [deg] | pressure $\theta_\sigma,\ \varphi_\sigma$ [deg] | value [B] |
| --- | --- | --- | --- | --- | --- |
| $\pi_{\mathrm{eff}}$ | Arbitrary in $X_1X_2$ plane | | Along $X_3$ | Along $X_1$ | 0.56 |
| $\delta'\varDelta_{k,\,\mathrm{max}}$ | Along $X_2$ | | Along $X_3$ | Along $X_1$ | 2.09 |
| $\delta'\varDelta_{k,\,\mathrm{min}}$ | 147 | 90 | Along $X_1$ | Along $X_1$ | 1.65 |
| $\delta'\varDelta_k$ | Along $X_2$ | | Along $X_3$: $n_{k,\,\mathrm{max}} = n_3$ <br> Along $X_1$: $n_{k,\,\mathrm{min}} = n_1$ | Along $X_1$ | 2.22 |

ence for the orthogonally polarized waves are realized in transversal geometry of interaction. The directions of applied pressure in all cases coincide with $X_1$ axis. Moreover the maxima of $\delta'\Delta_{k,\,max}$ and $\delta'\Delta_k$ are realized in the same geometries – in both cases the light wave must propagate along $X_2$ axis.

The separate contributions of the changes of the refractive indices $n_k$ and crystal thickness $t_k$ to the general piezo-optic effect, *i.e.*, the contributions of the first and the second term in the expressions for $\delta'\Delta_{k,\,max}$ and $\delta'\Delta_{k,\,min}$, can be estimated by the analysis of the surfaces for the objective functions containing one corresponding term only. For example, in Fig. 5 the mechanical stress extreme surfaces are built for the objective functions

$$\delta'\Delta_{k_1,\,max} \;=\; \sigma^{-1}\left|n_{k,\,max} - n_{k,\,max_0}\right| \tag{9}$$

$$\delta'\Delta_{k_2,\,max} \;=\; \sigma^{-1}(n_{k,\,max_0} - 1)\frac{|\delta t_k|}{t_k} \tag{10}$$

written on basis of Eq. (3).

As it is seen from Fig. 5, the extreme surfaces for these objective functions are essentially different: the extreme surface for the objective function $\delta'\Delta_{k_1,\,max}$ taking into account the refractive index changes only has got the "sphere-like" form, whereas the extreme surface for the objective function $\delta'\Delta_{k_2,\,max}$ taking into account the thickness changes has got the "parallelepiped" form. The maximum of the function $\delta'\Delta_{k_1,\,max}$ is equal to 1.46 B whereas the maximum of $\delta'\Delta_{k_2,\,max}$ is 2.98 B so both effects have got the comparable contributions to the total effect ($\delta'\Delta_{k,\,max}$). For instance, one can compare the influences of the contributions of $n_{k,\,max}$ and $t_k$ for the directions of the wave vector $\theta_k = 90°$, $\varphi_k = 90°$ and the applied pressure $\theta_\sigma = 90°$, $\varphi_\sigma = 0$ corresponding to the maximal piezo-optic effect, *i.e.*, the maximal value of the objective function $\delta'\Delta_{k,\,max} = 2.09$ B (see above). The objective functions (9) and (10) for these angles
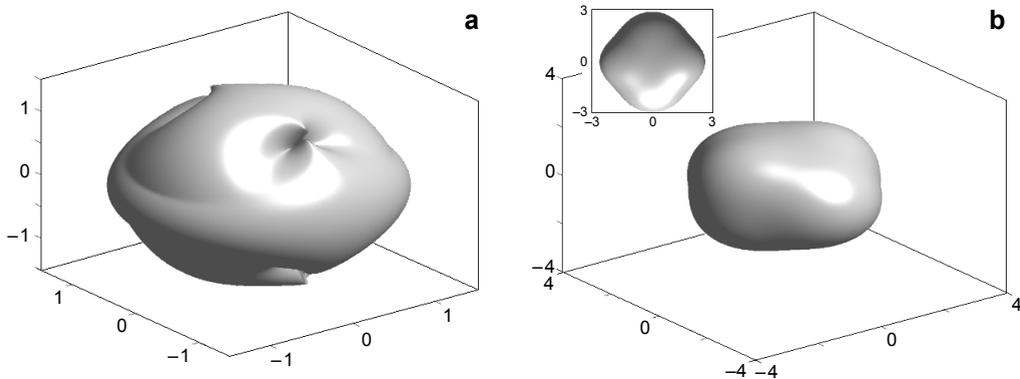


Fig. 5. The extreme surfaces of the mechanical stress (all values are in brewsters) for the objective functions $\delta'\Delta_{k_1,\,max}$ (**a**) and $\delta'\Delta_{k_2,\,max}$ (**b**); the top view of the surface is shown in insert in part **b**.

are equal to $\delta'\Delta_{k_1,\,max} = 1.46$ B and $\delta'\Delta_{k_2,\,max} = 0.63$ B correspondingly. So the contribution of the crystal thickness change is ~2.3 lower than the contribution of refractive index one in absolute value.

The analysis for the objective function $\delta'\Delta_{k,\,max}$ has got the analogous results.

As it follows from the results obtained earlier for lithium niobate crystal which is the well-known acusto-optical material [26], the maximal value of $\delta'\Delta_{k,\,max}$ for LiNbO$_3$ is approximately nine times higher than those calculated here for strontium borate and the maximal value of $\delta'\Delta_{k,\,min}$ is 4.5 times higher. However, the short-wavelength boundary of the transparency region of SrB$_4$O$_7$ is near 130 nm [15, 21, 27] whereas for LiNbO$_3$ it is observed at 300–400 nm depending on crystal doping and stoichiometry [28–30]. So strontium borate can be the effective material for interferometric light modulation in the UV region.

In the case of the objective function $\delta'\Delta_k$ describing the change in the optical path difference $\delta(\Delta n_k t_k)$ the general character of the extreme surface is close to the surface taking into account the changes of the refractive indices only (Fig. 5a). This peculiarity is caused by the character of the objective function determined by Eq. (8). Indeed, the birefringence for SrB$_4$O$_7$ is low (the maximal value of $\Delta n_k$ is 0.0033 [15]) and $|\delta t_k|/t_k \ll 1$, so the term $(n_{k,\,max_0} - n_{k,\,min_0})\,\delta t_k/t_k$ in the expression for $\delta'\Delta_k$ is low and $\delta'\Delta_k \approx \sigma^{-1}\big|(n_{k,\,max} - n_{k,\,max_0}) - (n_{k,\,min} - n_{k,\,min_0})\big|$. Thus the surface built for the objective function (8) is primary taking into account the changes of the refractive indices and, consequently, is similar to the one shown in Fig. 5a.

As it is also seen from this Fig. 5a, the extreme surface for $\delta'\Delta_{k_1,\,max}$ has got the distinctive peculiarity, the "teeth" at $\varphi_k = 90°$ that are also revealed on the other mechanical stress surfaces (Figs. 2b, 3b, and 4b). For better visualization of the "tooth", the part of the extreme surface cross-section is shown in Fig. 6 for the case of the objective function $\delta'\Delta_{k_1,\,max}$ (Fig. 5a) at $\varphi_k = 90°$. As it is seen from Fig. 6, the cross-section is divided in two parts divided by the angle $\theta_b = 33.4°$ corresponding to the angle between the longest axis of the optical indicatrix ($X_3$) and the binormal (optical axis). Because the values of the refractive indices for strontium borate are in agreement
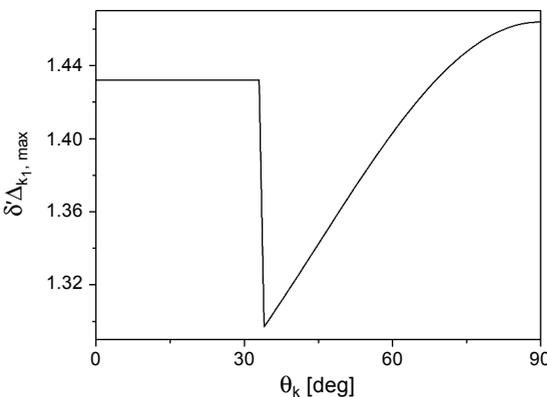


Fig. 6. The part of cross-section of $\delta'\Delta_{k_1,\,max}(\theta_k)$ surface at $\varphi_k = 90°$.

with the inequality $n_2 < n_1 < n_3$ (see Table 1), the binormals lie in $X_2X_3$ plane ($\varphi_k = 90°$). If the direction of the light beam is changed in this plane from $X_3$ axis ($\theta_k = 0$) to $X_2$ ($\theta_k = 90°$), the refractive index for the wave polarized along to $X_1$ is constant: $n(\theta_k) = n_1$. For the wave of the orthogonal polarization (in $X_2X_3$ plane), the refractive index increases from the lowest main value $n_2$ to the highest one $n_3$ at increasing of the $\theta_k$. At the angles $\theta_k < \theta_b$ the refractive index $n_{k,\,max} = n_1$ that corresponds to the initial part of the curve in Fig. 6 where the changes of $\delta'\Delta_{k_1,\,max}$ are relatively low. If $\theta_k > \theta_b$, the refractive index of the wave polarized in $X_2X_3$ plane exceeds $n_1$ and, consequently, it is chosen as $n_{k,\,max}$ by the computer program. Thus the "teeth" on the mechanical stress extreme surfaces are caused by passing of the wave vector **k** through the binormals of the strontium borate crystal.

## 5. Conclusions

For the case of the optically biaxial crystal of SrB$_4$O$_7$, the numerical optimization of the piezo-optic interaction geometry was carried out based on the construction of the special type ("extreme") surfaces. The objective functions for the optimization are the changes of the optical path for the waves of different polarization ($\delta'\Delta_{k,\,max}$, $\delta'\Delta_{k,\,min}$) and the propagation difference for the orthogonally polarized waves normalized on the value of mechanical stress and crystal thickness along the light propagation direction (direction of the wave vector) $\delta'\Delta_k$. The parameters of optimization are the angles determined by the direction of the applied uniaxial pressure (for the extreme surface of the mechanical stress) or light propagation (for the extreme surface of the wave vector).

As it is shown, the maximal achievable changes of the optical path induced by the mechanical stress are equal to 2.09 B (for $n_{max}$) and 1.65 B (for $n_{min}$) for the waves with orthogonal polarizations ($\lambda = 633$ nm) in the transversal geometry. The maximal propagation difference for the orthogonally polarized waves $\delta'\Delta_k$ is equal to 2.22 B in transversal geometry of interaction.

It is shown that the contributions of the changes of the sample thickness $t_k$ to the optical path changes $\delta'\Delta_{k,\,max}$, $\delta'\Delta_{k,\,min}$ is 2.3 times lower than the contribution of the refractive index changes. In the case of the objective function $\delta'\Delta_k$ the common effect is also caused by the changes of the crystal birefringence stipulated by the mechanical stress.

The comparison of obtained results with the ones for LiNbO$_3$ crystal shows that the maximal optical path length changes $\delta'\Delta_{k,\,max,\,min}$ for strontium borate ($\sim$3.5 B) are approximately four orders lower than for LiNbO$_3$. However, the advantage of SrB$_4$O$_7$ is its shortwave transparency (up to 130 nm) indicating that these crystals are perspective for the interferometric modulation of light in the ultraviolet spectral region.

## References

[1] SPILLMAN W.B., JR., *Multimode fiber-optic pressure sensor based on the photoelastic effect*, Optics Letters **7**(8), 1982, pp. 388–390.
[2] TRAINER N.N., *Photoelastic measuring transducer and accelerometer based thereon*, Patent 4.648.273 US, March 10, 1987.

[3] Andrushchak A.S., Mytsyk B.G., Osyka B.V., *Polarized-optical pressure meter*, Devices and Technique of Experiment, No. 3, 1990, p. 241 (in Russian).

[4] Baoliang Wang, *Linear birefringence measurement instrument using two photoelastic modulators*, Optical Engineering **41**(5), 2002, pp. 981–987.

[5] Xia S., Mello M., *Phase-multiplied photoelastic and series interferometer arrangement for full-field stress measurement in single crystals*, Experimental Mechanics **51**(4), 2011, pp. 653–666.

[6] Patel D., Veerasubramanian V., Ghosh S., Samani A., Qiuhang Zhong, Plant D.V., *High-speed compact silicon photonic Michelson interferometric modulator*, Optics Express **22**(22), 2014, pp. 26788–26802.

[7] Mytsyk B.G., Dem'yanyshyn N.M., *Piezo-optic surfaces of lithium niobate crystals*, Crystallography Reports **51**(4), 2006, pp. 653–660.

[8] Vlokh O.G., Mytsyk B.G., Andrushchak A.S., Pryriz Ya.V., *Spatial distribution of piezoinduced change in the optical pathlength in lithium niobate crystals*, Crystallography Reports **45**(1), 2000, pp. 138–144.

[9] Andrushchak A.S., Mytsyk B.G., Lyubych O.V., *Piezo-optic indicative surfaces in lithium niobate crystals*, Ukrainskii Fizicheskii Zhurnal **37**(8), 1992, pp. 1217–1224, (in Ukrainian).

[10] Demyanyshyn N.M., Mytsyk B.G., Andrushchak A.S., Yurkevych O.V., *Anisotropy of the electro-optic effect in magnesium-doped LiNbO$_3$ crystals*, Crystallography Reports **54**(2), 2009, pp. 306–312.

[11] Andrushchak A.S., Mytsyk B.G., Demyanyshyn N.M., Kaidan M.V., Yurkevych O.V., Dumych S.S., Kityk A.V., Schranz W., *Spatial anisotropy of linear electro-optic effect in crystal materials: II. Indicative surfaces as efficient tool for electro-optic coupling optimization in LiNbO$_3$*, Optics and Lasers in Engineering **47**(1), 2009, pp. 24–30.

[12] Andrushchak A.S., Chernyhivsky E.M., Gotra Z.Yu., Kaidan M.V., Kityk A.V., Andrushchak N.A., Maksymuk T.A., Mytsyk B.G., Schranz W., *Spatial anisotropy of the acousto-optical efficiency in lithium niobate crystals*, Journal of Applied Physics **108**(10), 2010, article 103118.

[13] Kaidan M.V., Tybinka B.V., Zadorozhna A.V., Andrushchak A.S., Schranz W., Sahraoui B., Kityk A.V., *The indicative surfaces of photoelastic effect in Cs$_2$HgCl$_4$ biaxial crystals*, Optical Materials **29**(5), 2007, pp. 475–480.

[14] Buryy O.A., Andrushchak A.S., Kushnir O.S., Ubizskii S.B., Vynnyk D.M., Yurkevych O.V., Larchenko A.V., Chaban K.O., Gotra O.Z., Kityk A.V., *Method of extreme surfaces for optimizing geometry of acousto-optic interactions in crystalline materials: example of LiNbO$_3$ crystals*, Journal of Applied Physics **113**(8), 2013, article 083103.

[15] Feng Pan, Guangqiu Shen, Ruji Wang, Xiaoqing Wang, Dezhong Shen, *Growth, characterization and nonlinear optical properties of SrB$_4$O$_7$ crystals*, Journal of Crystal Growth **241**(1–2), 2002, pp. 108–114.

[16] Vlokh O.G., Kityk A.V., Mokry O.M., Grybyk V.G., *Pressure–temperature phase diagram of (N(CH$_3$)$_4$)$_2$CuCl$_4$ crystals birefringent and elastic properties*, Physica Status Solidi (A) **116**(1), 1989, pp. 287–293.

[17] Furtak J., Czapla Z., Kityk A.V., *Ultrasonic studies of ferroelectric phase transition in Gly-H$_3$PO$_3$ crystals*, Zeitschrift für Naturforschung A **52**(11), 1997, pp. 778–782.

[18] Kaidan M.V., Zadorozhna A.V., Andrushchak A.S., Kityk A.V., *Cs$_2$HgCl$_4$ crystals as a new material for acoustooptical applications*, Optical Materials **22**(3), 2003, pp. 263–268.

[19] Kaidan M.V., Zadorozhna A.V., Andrushchak A.S., Kityk A.V., *Photoelastic and acousto-optical properties of Cs$_2$HgCl$_4$ crystals*, Applied Optics **41**(25), 2002, pp. 5341–5345.

[20] Press W.H., Flannery B.P., Teukolsky S.A., Vetterling W.T., *Numerical Recipes in Pascal*, 3rd Ed., Cambridge University Press, Cambridge, 2007, pp. 801–803.

[21] Demyanyshyn N.M., Mytsyk B.G., Sakharuk O.M., *Elasto-optic effect anisotropy in strontium borate crystals*, Applied Optics **53**(8), 2014, pp. 1620–1628.

[22] Mytsyk B., *Methods for the studies of the piezo-optical effect in crystals and the analysis of experimental data. I. Methodology for the studies of piezo-optical effect*, Ukrainian Journal of Physical Optics **4**(1), 2003, pp. 1–26.

[23] SIROTIN YU., SHASKOLSKAYA M., *Fundamentals of Crystal Physics*, "Mir", Moskow, 1982, (in Russian).

[24] MYTSYK B., DEMYANYSHYN N., MARTYNYUK-LOTOTSKA I., VLOKH R., *Piezooptic, photoelastic and acousto-optic properties of SrB$_4$O$_7$ crystals*, Applied Optics **50**(21), 2011, pp. 3889–3895.

[25] MARTYNYUK-LOTOTSKA I., DUDOK T., MYS O., VLOKH R., *Elastic, piezooptic and acoustooptic properties of SrB$_4$O$_7$ and PbB$_4$O$_7$ crystals*, Optical Materials **31**(4), 2009, pp. 660–667.

[26] MYTSYK B.G., ANDRUSHCHAK A.S., DEMYANYSHYN N.M., KOST' YA. P., KITYK A.V., MANDRACCI P., SCHRANZ W., *Piezo-optic coefficients of MgO-doped LiNbO$_3$ crystals*, Applied Optics **48**(10), 2009, pp. 1904–1911.

[27] OSELEDCHIK YU.S., PROSVIRNIN A.L., PISAREVSKIY A.I., STARSHENKO V.V., OSADCHUK V.V., BELOKRYS S.P., SVITANKO N.V., KOROL A.S., KRIKUNOV S.A., SELEVICH A.F., *New nonlinear optical crystals: strontium and lead tetraborates*, Optical Materials **4**(6), 1995, pp. 669–674.

[28] ARIZMENDI L., *Photonic applications of lithium niobate crystals*, Physica Status Solidi (A) **201**(2), 2004, pp. 253–283.

[29] SUGAK D.YU., MATKOVSKII A.O., SOLSKII I.M., KOPKO B.M., OLIINYK V.YA., STEFANSKII I.V., GABA V.M., GRABOVSKII V.V., ZARITSKII I.M., RAKITINA L.G., *Growth and optical properties of LiNbO$_3$:MgO single crystals*, Crystal Research and Technology **32**(6), 1997, pp. 805–811.

[30] SHASKOLSKAYA M.P., [Ed.], *Acoustic Crystals. Reference-Book*, Nauka, Moskow, 1982, (in Russian).